

Advanced Materials for Solid Oxide Fuel Cells

CONTRACT INFORMATION

Contract Number (FT) 22407

Contractor Pacific Northwest Laboratory
Operated for the
U.S. Department of Energy by
Battelle Memorial Institute
under contract DE-AC06-76RL0 1830
P.O. Box 999
Richland, Washington 99352
(509) 375-3938

Contractor Project Manager Dr. Timothy R. Armstrong

Principle Investigators Dr. Timothy R. Armstrong
Dr. Jeffry Stevenson
Dr. Steven Paulik

METC Project Manager W. Carey Smith

Period of Performance October 1, 1995 to July 30, 1996

Schedule and Milestones

FY 95 Program Schedule

	S	O	N	D	J	F	M	A	M	J	J	A
Interconnect Development												
High Performance Cathode												
Electrochemical Testing												
Accelerated Testing												

OBJECTIVES

The purpose of this research is to improve the properties of the current state-of-the-art materials used for solid oxide fuel cells (SOFCs). The objectives are to:

1. develop materials based on modifications of the state-of-the-art materials;
2. minimize or eliminate stability problems in the cathode, anode, and interconnect;

3. Electrochemically evaluate (in reproducible and controlled laboratory tests) the current state-of-the-art air electrode materials and cathode/electrolyte interracial properties;
4. Develop accelerated electrochemical test methods to evaluate the performance of SOFCS under controlled and reproducible conditions; and

The goal is to modify and improve the current state-of-the-art materials and minimize the total

number of cations in each material to avoid negative effects on the materials properties. materials to reduce potential deleterious interactions, (3) improve thermal, electrical. and electrochemical properties, (4) develop methods to synthesize both state-of-the-art and alternative materials for the simultaneous fabrication and consolidation in air of the interconnections and electrodes with the solid electrolyte, and (5) understand electrochemical reactions at materials interfaces and the effects of component composition and processing on those reactions,

BACKGROUND INFORMATION

Solid oxide fuel cells have emerged as a clean and efficient technology for the direct conversion of hydrogen and fossil fuels to electrical energy. The key feature of a SOFC is its high energy conversion efficiency, Compared with conventional methods of power generation, SOFCs offer several advantages: substantially higher conversion efficiency, modular construction, the potential for cogeneration, and much lower production of pollutants.

SOFCs are typically constructed using ceramic materials, Therefore, these fuel cells have several advantages over other types of fuel cells, specifically the use of nonprecious metals, solid state construction, and an invariant electrolyte. Ceramic fuel cells, however, place severe demands on the materials used due to their high operating temperature (1000°C) and the dual environments (oxidizing and reducing). Ceramic fabrication processes need to be developed to allow the incorporation of materials into practical stack configurations. At present, the key technical challenges for the development and commercialization of SOFCs are the development of suitable materials (specifically interconnect), improving the performance of the cathode/electrolyte interface and developing low-cost fabrication methods.

The principal components of a SOFC stack are the electrolyte, the anode, the cathode, and the interconnect. Each component serves several functions in the fuel cell and must meet certain

requirements, Each component must have the proper stability (i.e.. chemical, phase, morphological, and dimensional) in oxidizing and/or reducing environments, chemical compatibility with other components, and satisfactory conductivity. The components, in addition, must have similar coefficients of thermal expansion. The electrolyte and interconnect must be dense to prevent gas mixing, whereas the anode and cathode must be porous to allow gas transport to the triple phase boundary.

PROJECT DESCRIPTION

The overall approach to this research and development program is to:

1. Modify the current interconnect and cathode materials to minimize or eliminate stability problems, minimizing the number of cations in the composition to reduce potential deleterious interaction with other materials.
2. Electrochemically evaluate (in reproducible and controlled laboratory test) the current state-of-the-art air electrode materials and cathode/electrolyte interracial properties.
3. Develop methods to improve the air electrode/electrolyte interface through compositional modification. This will require modification of the interface with electronic, ionic, or mixed electronic/ionic conductors.
4. Develop accelerated electrochemical test methods to evaluate the performance of SOFCs under controlled and reproducible conditions.
5. Develop and test materials for use in low-temperature SOFCs. These materials need to be compatible with the new electrolytes, such as barium cerate, being developed.

RESULTS

Mechanical Properties of Acceptor Substituted Lanthanum Chromite

Acceptor-doped lanthanum chromite has been extensively studied over the past two decades as an interconnect material for high-temperature solid oxide fuel cells (SOFC). The interconnect is a critical component in a planar SOFC since, in addition to acting as the electrical connection between individual cells in series, it also must be gas tight in order to prevent mixing of the fuel and oxidizer. Only two materials, acceptor substituted lanthanum chromite and yttrium chromite, exhibit the required phase stability, high electronic conductivity, and low ionic conductivity in both reducing and oxidizing environments to be suitable as an interconnect material at high temperatures (1 000°C).

Several investigations have examined the strength of $\text{La}(\text{Ca})\text{CrO}_3$ and $\text{La}(\text{Sr})\text{CrO}_3$ as a function of various environmental conditions. Mori et al. [1] measured the 3-point bend strength of $\text{La}_{0.90}\text{Ca}_{0.10}\text{CrO}_3$ (LCC-10) and $\text{La}_{0.90}\text{Sr}_{0.10}\text{CrO}_3$ (LSC-10) at 25, 500 and 1000°C. LCC-10 showed a gradual decrease in strength with temperature, dropping to approximately 22% of the room temperature strength at 1000°C. LSC-10 showed a dramatic decrease in strength at 500°C (22% of room temperature) but remained relatively unchanged at 1000°C (29% of room temperature) (Figure 1). Milliken et al. [2] examined the effects of exposure to hydrogen ($\text{P}_{\text{O}_2} = 2 \times 10^{-18}$ atm) at 1000°C on the room temperature 4-point strength of $\text{La}_{0.83}\text{Sr}_{0.16}\text{CrO}_3$. The strength after exposure (up to 1000 h) was about 50% greater than that of the unexposed material. Montross et al. [3] measured the bend strength of LCC-15, LCC-20 and LCC-30 at 1000°C in air and in hydrogen. The strength of the LCC-15 and LCC-30 in hydrogen was significantly less than that in air while the LCC-20 relatively unaffected. Sammes et al. [4] have reported the most extensive strength testing to date. The 3-point bend strength of calender rolled LSC-15, LSC-20 and LSC-30 was measured at 25, 600, 700, 800, 900 and 1000°C. A gradual decrease

in strength with temperature was observed in all compositions (Figure 1). Additionally, the strength increased with increasing dopant content.

While these studies do suggest some trends between the materials, results of the individual studies are not consistent. It is difficult to make direct comparisons between studies since the sample dimensions vary widely as do the measurement method. Furthermore, no systematic study exists comparing not only the effects of temperature but also the effects of reducing environments, dopant and acceptor content.

Experimental Procedure

$\text{La}_{1-x}\text{Ca}_x\text{CrO}_3$ and $\text{La}_{1-x}\text{Sr}_x\text{CrO}_3$ powders were synthesized using the glycine nitrate process. Following synthesis, powders were calcined at 1000°C for 1 hour in air. Due to the particle morphology (hard agglomerates, high surface area, low packing density) the powder was isostatically pressed into bars at 276 MPa. These bars were ground using a mortar and pestle and sized until the powder was less than 100 mesh. The powder was then again isostatically pressed into billets, approximately 34 mm by 34 mm by 64 mm. The green density of these billets was 65 to 68 % of theoretical. The green billets were sintered in air between 1550 and 1690°C for 2 to 6 hours. Selected billets were machined into 3 mm by 4 mm by 45 mm bars (Bomas Machine Specialists) according to military standard 1942B. Additionally, one billet of each composition was sectioned into 10 mm thick samples and polished for fracture toughness and elastic modulus measurements.

The elastic modulus was measured using a pulse-echo technique on the polished samples. Using a 50 MHz longitudinal and a 25 MHz transverse transducer, hooked up to a computer data acquisition system, the transit time for a given pulse to traverse through a sample was measured.

Four point bend strength was measured (Instron Model 1125) with a crosshead speed of 0.508 mm/min on a 20 mm top and 40 mm

bottom span. Tests were carried out in air at 25, 600, 800 and 1000°C. Samples were heated at approximately 20 to 25 °C/min and allowed to equilibrate for 15 minutes at temperature prior to testing,

Selected samples were heated to 1000°C in air in a silica tube furnace and allowed to equilibrate for 15 minutes. After which the oxygen partial pressure $P(O_2)$ was changed. Measurements as a function of the $P(O_2)$ were carried out using a buffered $CO_2/Ar/H_2$ gas system, enabling expansion measurements to be made over an oxygen partial pressure range from 10^{-5} to 10^{-18} atmospheres at 1000°C. To ensure complete mixing of the gases, flow rates of 300 seem were used. During cooling, constant $P(O_2)$ was maintained to 700°C by adjusting the ratio and flow of the gases. The treated bars were then fractured in air at room temperature.

Scanning electron microscopy was used to analyze the fracture surfaces of all samples to look for changes in fractures, secondary phases, and changes in the microstructure that may have occurred during reduction.

Results

The bend strength of the LCCS as a function of temperature is shown in Figure 2. Each data point represents an average of 10 tests, while the error bars indicate one standard deviation. The initial trend in bend strength with acceptor content was $LCC-25 > LCC-20 > LCC-15$. The data, however, indicated that the bend strength of LCC-30 was less than that of LCC-20, suggesting significant changes in the microstructure and/or fracture mechanisms within this sample. All samples displayed a reduction in strength at 600°C. The strength of LCC-30 decreased linearly with temperature to 1000°C, while the LCC-25 showed a small decrease in strength from 600 to 1000°. The strength of the LCC-20 remained essentially constant from 600 to 1000° and LCC-15 showed an increased with temperature to 1000°, These trends are more clearly shown in Figure 3. This figure shows the fracture strength as a function of temperature referenced to the room

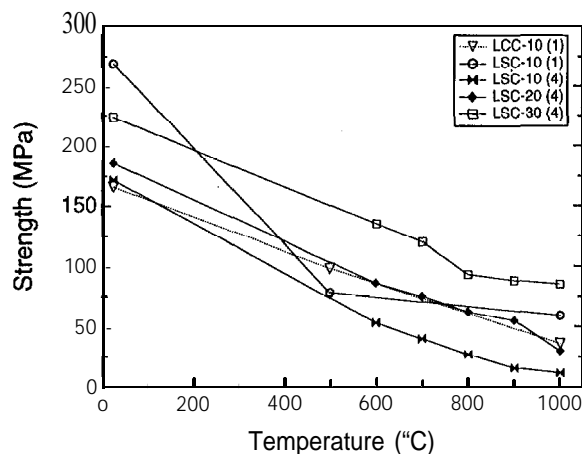


Figure 1. Strength of LSC and LCC with temperature

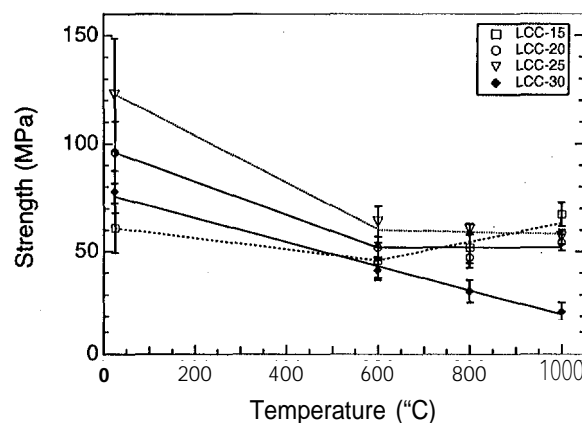


Figure 2. Strength of glycine nitrate synthesized LCC with temperature.

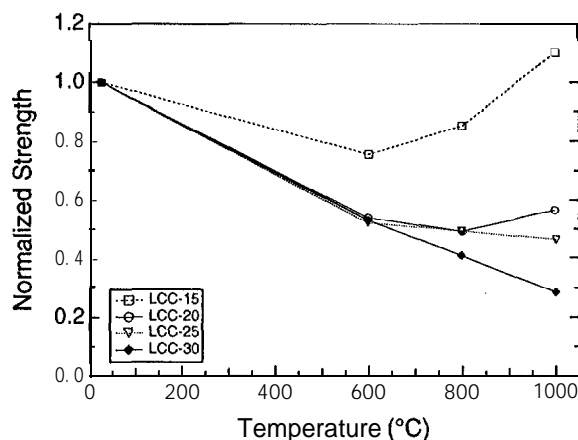


Figure 3. Normalized strength of LCC.

temperature fracture strength. The data displayed clearly shows that the decrease in decreasing acceptor content in the chromite. In strength with temperature decreases with addition LCC-15 and LCC-20 show an increase in strength with temperature. This increase in strength observed at high temperature is similar to measurements of UO_2 , where the strength was found to increase due to extension of existing flaws (pores) in the sample. [6]

The fracture strength of LSC as a function of temperature is shown in Figure 4. The room temperature fracture strength of the LSCS showed a similar increase in strength with acceptor content (Figure 4). However, the LSCS demonstrated no change in strength with temperature.

Figure 5 depicts the change in room temperature bend strength of LCC-20, LCC-25 and LCC-30 after exposure to high temperature (1000°C) reducing conditions. Both LCC-25 and LCC-30 showed essentially no change in strength to moderately reducing environments (10^{-8} and 10^{-10} atm). However, at lower oxygen partial pressures, the strength decreased rapidly with decreasing P_{O_2} , to 10^{-6} atm. The strength of the LCC-20 was constant up to a P_{O_2} of 10^{-12} , but again dropped rapidly with decreasing P_{O_2} . The oxygen partial pressures where the initiation of the decline in strength was observed agrees with previously reported effects of reduction on oxygen stoichiometry [7]. In addition, the decrease in strength parallels reported decreases in electrical conductivity and increases in the expansion of these materials, which have been directly related to the oxygen content of the samples [8, 9].

The electroneutrality relation for acceptor-doped lanthanum chromite can be written (using Kroger-Vink notation [10]) as:

$$[\text{A}'_{\text{La}}] = [\text{Cr}^{\bullet}_{\text{Cr}}] + 2 [\text{V}^{\bullet\bullet}_{\text{O}}]$$

where the brackets refer to concentration expressed in mole fractions, A represents Sr or Ca, "•" represents unit negative charge with respect to the LaCrO_3 lattice, "••" represents

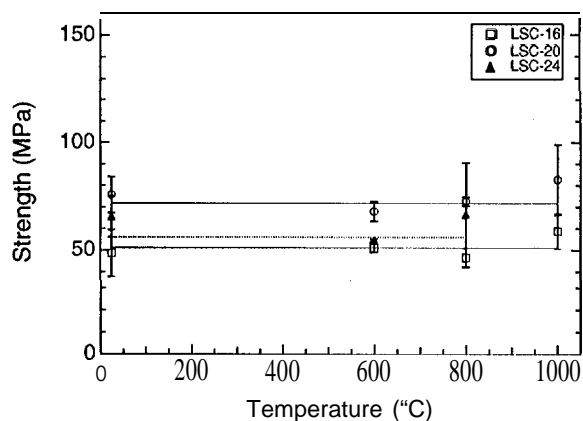


Figure 4. Strength of glycine nitrate synthesized LSC with temperature.

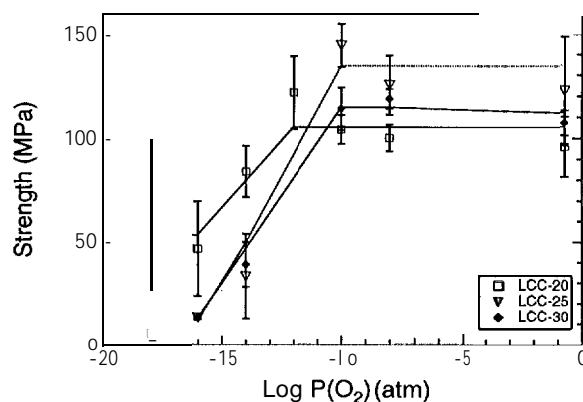


Figure 5. Room temperature fracture strength of LCC samples exposed to the indicated oxygen partial pressures for 2 hours.

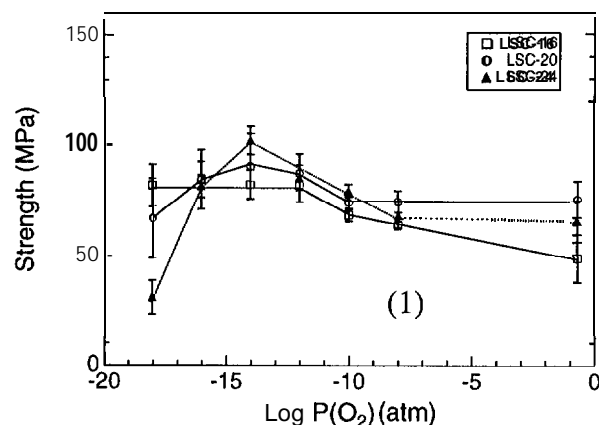
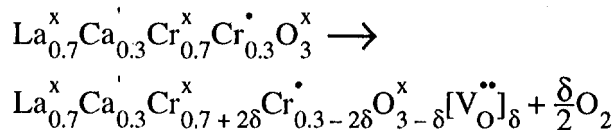
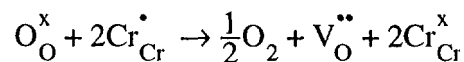


Figure 6. Room temperature fracture strength of LSC samples exposed to the indicated oxygen partial pressures for 2 hours,

unit positive charge with respect to the lattice, and V_O refers to oxygen vacancies, Since the acceptor concentration remains constant for a given material, electroneutrality requires that the formation of oxygen vacancies under reducing conditions results in a simultaneous decrease in the concentration of $Cr^{4+}(Cr^\bullet)$:



Simplification to eliminate nonparticipating species yields:



where “ x ” refers to neutrality with respect to the lattice (so that $Cr^x = Cr^{3+}$). In the equation, δ represents the oxygen vacancy concentration, $[V_O^{\bullet\bullet}]$, expressed as a mole fraction.

SEM analysis of the fracture surface of as-sintered LCC-30 indicated the sample failed by intergranular fracture. Observation of samples treated in reducing in environments indicated a change in fracture mechanism,

Conclusions

Room temperature bend strengths tend to increase with increasing dopants content, for both the LCC and YCC materials. Relative to room temperature values, the proportional decrease in high temperature strengths of the LCCS increased with increasing acceptor content. The strength of the YCCS increased slightly with temperature. The room temperature bend strength of the LCC-25 and LCC-30 remained constant after exposure to moderately reducing high temperature condition but dropped precipitously at 10^{-14} and decreased further at 10^{-16} atm PO_2 . For YCC-20, the room temperature bend strength was invariant until a precipitous drop occurred at 10^{-16} . The drastic decrease in bend strength was accompanied by a

change in fracture mechanism as transgranular fracture was observed.

LSC samples exposed to the indicated oxygen partial pressures for 2 hours.

The critical partial pressure increases with increasing temperature. Significant amounts of secondary chromate phase may enhance the expansion upon reduction. Another plausible explanation is that the composition of the sample may be closer to LSC-24 than LSC-20 as indicated by the similarity of data in Figure 4.

References

1. M. Mori, H. Itoh, N. Mori and T. Abe, in Proceedings of the Third International Symposium on Solid Oxide Fuel Cells (1993); Edited by S.C. Singhal and H. Iwahara, 325-334.
2. C. Milliken, S. Elangovan and A. Khandkar, in Proceedings of the Third International Symposium on Solid Oxide Fuel Cells (1993); Edited by S.C. Singhal and H. Iwahara, 335-343.
3. C.S. Montross, H. Yokokawa, M. Dokiya and M. Anzai, in Extended Abstracts of the 60th meeting of the Electrochemical Society of Japan (1993), 263,
4. N.M. Sammes, R. Ratnaraj and C.E. Hatchwell, in Proceedings of the Fourth International Symposium on Solid Oxide Fuel Cells (1995); Edited by M. Dokiya, O. Yamamoto, H. Tagawa and S.C. Singhal, 952-959.
5. G.D. Quinn, F.I. Baratta, and J. A. Conway, Army Materials and Mechanics Research Center Technical Report 85-21, 1985.
6. R. W. Davidge, Mechanical Behavior of Ceramics, Cambridge University Press, Cambridge England (1979). “

7. J. Misusaki, S. Yamauchi, K. Fueki, and A. Ishikawa, Solid State Ionics, 12, (1984) 119.
8. I. Yasuda and T. Hikita, J. Electrochem. Soc., 140 (1993) 1699.
9. T. R. Armstrong, J. W. Stevenson, L. R. Pederson, and P. E. Raney, J. Electrochem. Soc., (1996).
10. F.A. Kroger, The Chemistry of Imperfect Crystals, North-Holland, Amsterdam, (1964)